Photodetachment of Ferrocyanide in Reverse Micelles

Gerald M. Sando[†] and Jeffrey C. Owrutsky*

Code 6111, US Naval Research Laboratory, Washington D.C. 20375-5342

Received: November 17, 2005; In Final Form: February 15, 2006

Solvated electrons have been generated in reverse micelles (RMs) through photodetachment of ferrocyanide ($Fe(CN)_6^{4-}$) in sodium bis(2-ethylhexyl) sulfosuccinate (AOT) RMs. We have measured both bleach recovery of the parent ferrocyanide CN stretch in the infrared and the decay of the solvated electron absorption at 800 nm. The bleach recovery has been fit to a diffusion model for the geminate recombination process. The fit parameters suggest a narrowing of the spatial distribution of ejected electrons due to confinement in the RMs when compared to bulk water. The diffusion coefficient of the solvated electron does not appear to be significantly affected by RM confinement. The decay of the solvated electron absorption exhibits an additional decay component that is not observed in bulk water and is smaller for larger RMs. No corresponding additional component is seen in the parent ferrocyanide IR bleach recovery, which supports our interpretation that the confinement-induced new decay process in RMs is due to electrons reacting with AOT headgroups.

Introduction

The nanosized pools of water formed in the cores of reverse micelles (RMs) offer a convenient way to study the effects of spatial confinement on chemical dynamics and reactivity. RMs provide an easy method of controlling the extent of confinement because the RM radius is determined by the molar ratio of water to surfactant, $\omega = [H_2O]/[\text{surfactant}]$, and is often a nearly linear function of ω.[1,2] The solvated electron is an example of a system that may exhibit interesting changes due to spatial confinement. Electrons in water continue to be a system of widespread research interest.[3] Extending bulk water studies of electron reactivity and charge-transfer reactions to more complex aqueous environments, such as confined or interfacial water, is important due to its relevance to biological systems.[3] Solvated electrons have been formed in reverse micelles by photoionizing the organic solvent[4,5] or aromatic electron donors at the interface[6,7] as well as by radiolysis.[8−14] Experiments have shown a spectral shift of the solvated electron absorption for small RMs, although for large enough RMs ($\omega \sim 20$) the absorption spectrum is identical to that in bulk water.[7,8,11,14] This suggests that the solvation environment of the electron is perturbed upon confinement only for small RMs. This is not surprising due to the small size (~3 Å) of the solvent cavity formed by the solvated electron.[15] The rate of attachment of electrons to RMs after photoionization of the organic phase depends on RM size more than is predicted by diffusion.[5] This dependence has been attributed to confinement effects on the excited states of the electron in water, some of which have a larger spatial extent than a ground state solvated electron. These studies are possible because electrons have lifetimes of only a few picoseconds in organic solvents, but have microsecond lifetimes in aqueous solution. In related studies, the photoreactivity of the excited solvated electron with surfactant headgroups has been studied in RMs and it exhibits a size dependence consistent with confinement effects on the delocalized excited state of the electron.[4]

A popular method of generating solvated electrons in bulk water is through anion photodetachment. This has the advantage over photoionization of water in that photodetachment can be a single photon process while water photoionization is usually a multiphoton process. Anions that have been used in photodetachment studies include halides,[16−22] hydroxide (OH^-),[23] and ferrocyanide ($Fe(CN)_6^{4-}$).[24−28] The distribution of electron ejection distances can be determined from the geminate recombination dynamics of these systems. For the monovalent anions, the electrons and the neutral radical parent appear to form a short-lived (~10 ps) caged pair.[17−19,23,29] In the case of ferrocyanide, single photon ionization at 255 nm resulted in ~15 Å ejection distances based on diffusional modeling of the geminate recombination dynamics.[24] For the photoionization of water, the average ejection distance depends on the excitation energy, ranging from ~10 Å to >50 Å, with higher energy excitation resulting in larger distances.[30] In general, the solvated electron is not initially created in its final thermalized state. Instead, the initial "presolvated" electron relaxes rapidly, which is accompanied by solvent reorganization, both of which lead to spectral shifts and result in the thermalized ground-state solvated electron.[15,16,24,25,31−35] A detailed understanding of the presolvated electron states has not been achieved yet, but it is generally agreed that they are somewhat delocalized and depend on the electron formation method.[15,30,31] It is the relaxation of the delocalized presolvated state that leads to the spatial distribution of solvated electrons.

Generating solvated electrons within a RM water pool poses some additional challenges and complications compared to bulk water. Photoionization of neutral aromatic molecules has been used to create solvated electrons within RMs, but these electron donors are most likely located on the nonpolar side of the interface.[6,7] The initial dynamics and the geminate recombination partner are outside of the RM water pool, limiting the information that can be obtained about electrons in the RM core. Direct photoionization of water inside the water pool poses other problems due to the presence of the organic phase. Both water and the organic phase are susceptible to multiphoton ionization, and since the organic phase is in excess, most of the electrons

* To whom correspondence should be addressed. E-mail: jeff.owrutsky@nrl.navy.mil.

[†] NRL-ASEE Research Associate.

10.1021/jp056667v CCC: $33.50
Published on Web 04/27/2006

will originate from the organic phase.[5] This suggests that anion photoionization is the most promising method, but the presence of the surfactant can limit the range of UV excitation. This is especially true for surfactants with an aromatic group. Even in the case of single photon detachment, the pump power must be kept low because the organic solvent can undergo fairly facile multiphoton ionization at wavelengths suitable for photodetachment.

Solvated electron formation through photodetachment of ferrocyanide in AOT (sodium bis(2-ethylhexyl) sulfosuccinate) RMs avoids most of these pitfalls. Ferrocyanide is stable in AOT RMs.[36] Although AOT RMs are well characterized,[1,2,37−41] the addition of ferrocyanide reduces the stability of the RMs to a fairly narrow range ($\omega = 5-14$), and the ferrocyanide concentration in the aqueous phase must be kept relatively low (~0.1 M).[36] In addition, AOT has a low absorption at 267 nm, a wavelength that is conveniently produced via third harmonic generation of a Ti:Sapphire laser for photodetaching ferrocyanide in a one photon process. Ferrocyanide has a large negative charge, resulting in high hydrophilicity and an increased tendency to reside in the RM water pool. This is consistent with IR spectroscopic studies in RMs that suggest that ferrocyanide resides in the center of the RM water pool.[36] The average ejection distance in bulk water is 15 Å,[24] which is on the order of the RM water pool radii of 16 Å and 22 Å for $\omega = 8$ and 12, respectively.[1] The initial excited state is delocalized over several solvent spheres.[15,24,25] Therefore, we anticipate observing confinement effects on the presolvated electron that result in changes in the electron spatial distribution. In addition, the strong CN band of ferrocyanide permits one to follow the bleach and recovery of the parent ferrocyanide in the IR in addition to the solvated electron absorbance at 800 nm. This allows clearly distinguishing between geminate recombination and other electron decay pathways.

Although changes in the initial electron trapping and relaxation dynamics are likely, in this study we concentrate on the geminate recombination process to determine changes in the electron distribution and reactivity. Confinement in a RM results in a geminate recombination rate that depends on the RM size, with faster recombination observed for a smaller RM. In addition, we observe an additional decay pathway for the electron that appears to be quenching of the electron by the surfactant. There is, again, a size dependence with a more pronounced and faster additional component for smaller RMs. Quenching by AOT has been observed for electrons produced in the organic phase for dry RMs,[8] but this is the first report of quenching by AOT for electrons produced in the water pool.

Experimental Section

Details of the laser system can be found in a previous publication.[42] Briefly, the laser system consists of a titanium sapphire oscillator pumped by a CW Nd:VO_4 laser. The oscillator output is amplified in a regenerative amplifier (regen) pumped by a Nd:YLF laser providing ~100 fs pulses with an energy of ~900 μJ at 1 kHz near 800 nm. About 300 μJ of the regen fundamental is frequency tripled to produce 2−20 μJ UV pump pulses near 267 nm. The UV pump intensity is controlled by a half-waveplate in the frequency tripler. A small portion of the fundamental is split off for a 800 nm probe pulse. Mid-IR pulses are produced through difference frequency generation of the signal and idler of an optical parametric amplifier. The probe beams are directed to translation stages to control the delay time and then to the sample. The IR probe is sent through a monochromator with ~5 cm^{-1} resolution. The transmitted signals are detected with either a HgCdTe infrared detector combined with a gated integrator for the IR probe or a photodiode for the 800 nm probe. The probe signals are processed with a pair of lock-in amplifiers to determine the absorbance change ($\Delta A(t) = \log[T_{unpumped}/T_{pump}(t)]$). The polarization of the pump and probe beams were parallel. The pump and probe beam diameters were 310 μm and 150 μm, respectively. The alignment of both probe beams through the translation stages was checked by monitoring the transmission through a 100 μm pinhole where the transmission decreased by less than 3% over the delay (300 ps) investigated in the experiment.

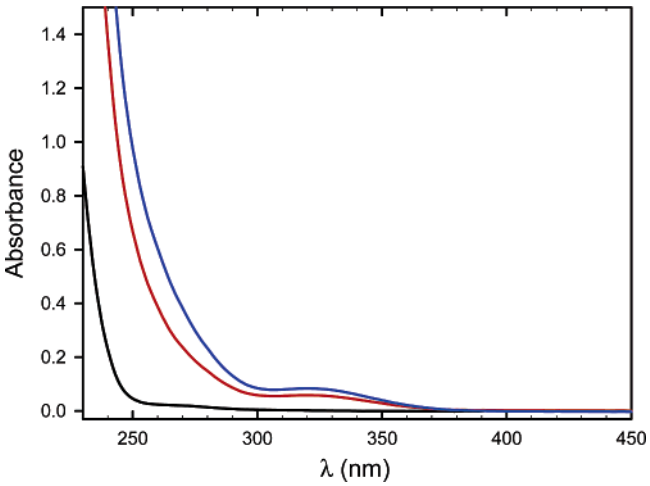

Figure 1. UV−Visible absorption spectra of $\omega = 8$ (red) and 12 (blue) AOT RMs with 0.1 M ferrocyanide in the aqueous phase and $\omega = 12$ without ferrocyanide (black).

RM solutions were prepared using 0.25 M NaAOT (Aldrich 98%, used as received) in isooctane. Isooctane was used to minimize multiphoton signals due to the organic solvent, which are larger for heptane and cyclohexane. Potassium ferrocyanide was added as a 0.1 M aqueous solution into the surfactant solutions to reach the proper ω. The samples were sonicated until a clear solution resulted. Under these conditions the aggregation numbers (surfactant molecules per RM) should be near 100 for $\omega = 8$ and 12,[43] resulting in a RM concentration of 0.0025 M and ~2 ferrocyanide molecules per RM. Samples were flowed in a Harrick cell with 500 μm spacers. Bulk water studies were performed using 25 μm spacers. Nitrogen purging of the solutions resulted in no change in sample kinetics.

Results

The UV−visible spectra of the RMs systems studied are shown in Figure 1. Spectra are shown both with and without ferrocyanide. The ferrocyanide containing samples show a large increased absorption in the UV region below 300 nm as well a smaller absorption band near 330 nm. After subtracting the appropriate background spectra, we estimate an extinction coefficient, ϵ_{267}, of 1400 $M^{-1}cm^{-1}$ for ferrocyanide in both RMs ($\omega = 8$ and 12) at the excitation wavelength of 267 nm, consistent with the previously reported bulk water value.[44] The IR spectra in the CN stretch region agree with the previously reported spectra using *n*-heptane as the nonpolar phase with a small (<1 cm^{-1}) dependence of the vibrational frequency on ω.[36] We estimate a peak extinction, ϵ_{IR}, of 4100 $M^{-1}cm^{-1}$ for the CN band, which is centered near 2038 cm^{-1}.

The transient kinetics and their respective fits (described in text) are shown in Figure 2. The decays are normalized at 10 ps, after the electron thermalization is complete and before

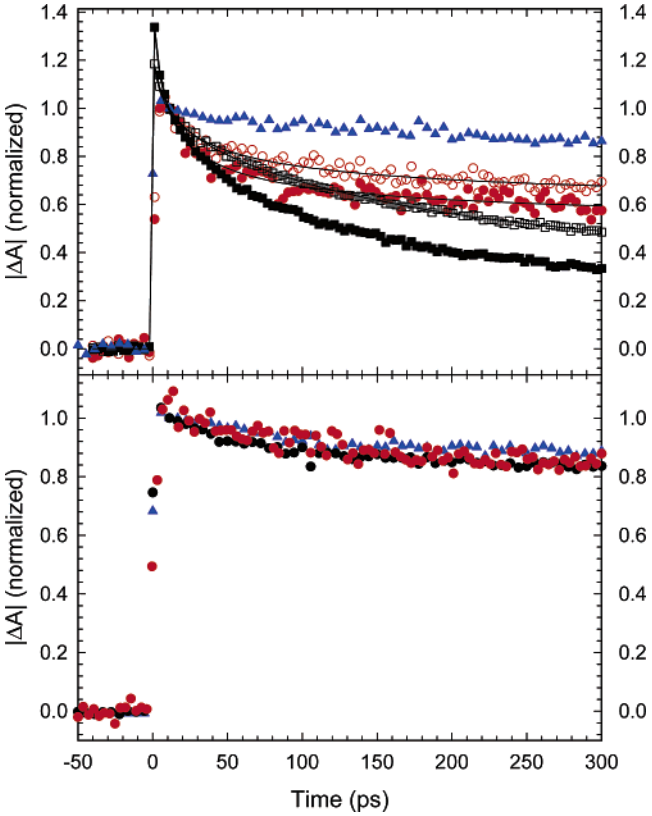

Figure 2. (Top) Transient bleach of the ferrocyanide CN stretch near 2038 cm^{-1} for $\omega = 8$ (filled red circles) and 12 (open red circles) AOT RMs. Transient absorption at 800 nm for ferrocyanide in $\omega = 8$ RMs (solid black squares) and $\omega = 12$ RMs (open black squares). Transient absorption at 800 nm for AOT RMs containing only water (blue triangles). Fits of the ferrocyanide containing RM data (see text) are included as solid lines. (Bottom) Transients absorptions at 800 nm for ferrocyanide in bulk water (blue triangles) and 2.75 M NaCl (black circles). Transient bleach for ferrocyanide in bulk water near 2038 cm^{-1} (red circles). All transients are normalized at 10 ps, after electron thermalization and before any significant recombination.

significant recombination occurs. No dependence on polarization is expected for the transient absorption of the electron[45−47] or the bleach of the triply degenerate T_{1u} CN mode of ferrocyanide, so no polarization dependent studies were undertaken. Any unexpected anisotropy should decay before the time window of interest (>10 ps). The bleach of the parent ferrocyanide CN stretch at 2038 cm^{-1} is shown for $\omega = 8$, $\omega = 12$, and bulk water. The data presented are an average of several scans with pump powers between 4 and 8 μJ and were power independent in this regime. Higher pump powers distorted the early time (<50 ps) data due to interference from a large early time absorption that appeared in all samples, as previously observed in bulk water.[25,32] Very little bleach recovery is seen in bulk water with ~90% of the signal remaining at 300 ps, consistent with previous studies.[24,25] In the RMs, significantly more bleach recovery is observed. The signal at 300 ps is down to <70% for $\omega = 12$ and <60% for $\omega = 8$ of the initial signal.

The decay of the solvated electron population was followed using the transient absorption at 800 nm. In bulk water the kinetic behavior of the solvated electron absorption is the same as the ferrocyanide bleach within experimental error, with ~90% of the initial signal remaining at 300 ps. The addition of 2.75 M NaCl results in slightly more solvated electron decay, with ~85% remaining at 300 ps. The two-photon detachment of Cl^- is negligible under our pump conditions. For the RMs, the electron signal decays more rapidly than the ferrocyanide bleach recovers. The electron absorption decays to 50% of the initial signal for $\omega = 12$ and to 33% for $\omega = 8$ at 300 ps. The data shown is an average of several scans with pump pulse energies of 2 or 4 μJ (2.7 to 5.3 mJ/cm^2 for 310 μm diameter pump). The transients were pulse energy independent in this regime, and higher pump energies resulted in slower decays. There is a larger difference between the IR bleach recovery and 800 nm absorption decay for $\omega = 8$ than for $\omega = 12$. The signals observed after 10 ps using a 615 nm probe (not shown) from second harmonic generation of the OPA output were indistinguishable from those with the 800 nm probe pulses. Differences due to solvation were evident in the early time data (<5 ps), but no spectral evolution was evident over the time scale of interest. Also shown is the 800 nm transient absorption signals for RMs that do not contain ferrocyanide using 16 μJ pump pulses. The higher powers are necessary for acceptable signal-to-noise for the multiphoton process. These showed no ω dependence for $\omega \geq 8$, and these scans at several ω values were averaged to reduce noise in the presented data. There was a small decay in the 800 nm absorption such that ~88% of the initial signal remains at 300 ps. Addition of CCl_4 as an electron quencher in the organic phase (not shown) resulted in a disappearance of nearly all of the 800 nm absorption for RMs without ferrocyanide, but resulted in little change in the 800 nm absorption for ferrocyande containing RMs. There was evidence of long-term photoproduct for the ferrocyanide containing RMs when CCl_4 was added, and this prevented measurement of low noise data. The signal amplitude slowly decreased over time and translation of the sample resulted in recovery of the full signal.

Discussion

Solvated Electron-Generation and Early Time Behavior. The nature of the precursors to the solvated electron has been a source of controversy.[15,16,24,31−33,46,48−54] This is primarily due to the short lifetime and broad spectral features of the presolvated electron. Spectral features have been observed over a broad spectral range, ranging from the visible to mid-infrared, complicating efforts to achieve a comprehensive characterization. The nature of the precursor also appears to depend on the method used to generate the solvated electron.[15,29,31] The early time dynamics of the electron not only includes electronic relaxation, but also spectral shifts due to solvation dynamics as the solvent reorients in response to the electronic relaxation of the electron. Despite these difficulties, it is generally agreed that the precursor is delocalized in the case of ferrocyanide photodetachment. Strong evidence for this has been provided by results of static quenching studies[15] as well as from a determination of the average ejection distance of 15 Å.[24] Since this distance is on the order of the RM size (radii of 16 Å and 22 Å for $\omega = 8$ and 12, respectively), it should be expected that the electron relaxation process will be affected by RM confinement. However, most of these processes are too fast to resolve using our current apparatus. The extremely fast and complex nature of the initial relaxation dynamics, which become more complex in a RM where there may be additional early time dynamics due to multiphoton excitation of the organic solvent, has led us to concentrate on the dynamics after electron thermalization. This includes changes in the geminate recombination process due to altered electron distributions and any changes in the reactivity of the electron on the time scale of tens to hundreds of picoseconds.

Signal Origin. Solutions that form RMs contain nonpolar organic solvents as the major component. Most organic solvents

commonly used in RMs, generally hydrocarbons, undergo multiphoton ionization in the near-UV.[55−57] The free electrons then quickly attach to RM water pools and would interfere with studies of photodetachment of anions within the water pool. In addition, excited states or ionized hydrocarbons can absorb at 800 nm, the wavelength of our probe used to monitor the solvated electron population. To investigate confinement effects on electron behavior in water, it is critical for us to generate the electrons in the water pool. In addition, our measured signals must be due to the solvated electrons rather than from ionized organic solvent. Our initial studies used *n*-heptane as the nonpolar phase and the 800 nm probe results appeared to have a significant contribution from the organic phase with power dependent kinetics, as would be expected when one- and two-photon processes are competing. There are reports that suggest isooctane photoionization results in smaller signals near 800 nm than for photoionization of linear hydrocarbons.[55−57] For these reasons, we changed our nonpolar phase to isooctane to minimize contributions from the organic component.

For a constant pump power, inclusion of ferrocyanide in the RM results in a much larger transient absorption at 800 nm than without ferrocyanide. Including ferrocyanide also results in significant absorption of the pump, leaving less pump power to induce the multiphoton absorption of isooctane. In addition, the decay characteristics of the system change when ferrocyanide in included. In the absence of ferrocyanide, little decay is observed over a 300 ps time window while significant decay is evident with ferrocyanide. Since the concentration of ferrocyanide is kept constant in the aqueous phase, we would expect the multiphoton signal to be larger for the $\omega = 8$ RMs than for the $\omega = 12$ RMs since less pump is absorbed by ferrocyande in the former. If isooctane ionization had a significant contribution to the 800 nm signal, we would expect the absorption to have a slower decay for $\omega = 8$, but the opposite result is observed. The 800 nm absorption decays were power independent for pump energies of ≤ 4 μJ, but the decays slowed when pump energies were much larger than 4 μJ, consistent with the onset of ionization of the organic phase. To provide further evidence of the origin of the 800 nm absorption, we added CCl_4 as electron quencher to the organic phase.[55] The addition of quencher had little, if any, effect on the ferrocyanide containing RMs (not shown). On the other hand, inclusion of CCl_4 in the RMs without ferrocyanide resulted in negligible 800 nm probe signals. This indicates that the vast majority (>90%) of our 800 nm signal results from solvated electrons photodetached from ferrocyanide.

For our infrared signals the situation is much more clear. We observe a strong absorption in the IR that decays to zero within a few ps and shows no significant frequency dependence. This signal is observed in every sample we have studied regardless of ferrocyanide or water content. It is also observed in neat hydrocarbons. This absorption increases in intensity upon inclusion of ferrocyanide. This absorption is consistent with previous studies and is attributed to a presolvated electron in the aqueous phase[25,32] or an electron in the nonpolar phase.[55] After a few ps, no IR transient signal remains except for a bleach of the ferrocyanide CN stretch for ferrocyanide containing samples. This transient bleach is only observed at the frequency of the ferrocyanide CN stretching band.

Ferrocyanide Bleach Dynamics (IR). We have established that, after a few ps, the IR transient signal is due to the bleach of the ferrocyanide CN band. As shown in Figure 2, the ferrocyanide bleach recovery has a significant dependence on the sample conditions, with a much larger recovery in the RMs than in bulk water. The most likely source of the bleach recovery is geminate recombination between the solvated electron and the oxidized parent. The reaction rate between ferricyanide ($Fe(CN)_6^{3-}$), the product that results from removing an electron from ferrocyanide, and the electron is known to be diffusion limited.[24,58] To quantify the kinetics, we have fit the IR data to a diffusion survival probablility model. Recombination between electrons and ferricyanide in bulk water has been shown to be well described by the diffusion equation.[24] However, diffusional recombination of two charged species requires the inclusion of an electrostatic potential between the recombination partners, preventing an analytic solution to the diffusion equation. Ferrocyanide undergoes ion pairing with the K^+ counterions that depends on ionic strength,[59] so the electrostatic potential for diffusion can be modeled as a Coulomb potential between the electron and the average charge on ferricyanide.[24] At high enough ionic strength, the ion pairing is strong enough to assume that ferricyanide is neutral, removing the electrostatic potential and allowing an analytical expression for the survival probability assuming a Gaussian distribution of electrons. This assumption was shown to be valid for 0.4 M ferrocyanide in a previous study of recombination in bulk water.[24] In the RMs the concentration of ferrocyanide was 0.1 M in the aqueous phase. There is also an unknown amount of dissociated Na^+ counterions from AOT. If completely dissociated, this would be 6.9 M in Na^+ for the $\omega = 8$ RMs. Combining the unknown extent of dissociation of AOT with the fairly high concentration of ferrocyanide, we have chosen to assume that the ion pairing is strong enough to use the neutral ferricyanide approximation and the analytical recombination expression.

The simplest model assumes that the recombination partners are created in solution at a distance of r_0. The two species then undergo three-dimensional diffusion. We also assume that the species recombine instantaneously if they come within the reaction distance, r_{xn}. Under these assumptions, the survival probability is[18]

$$\Omega(r_0,t) = 1 - \frac{r_{xn}}{r_0} erfc\left(\frac{r_0 - r_{xn}}{\sqrt{4D't}}\right) \qquad (1)$$

where D' is the sum of the diffusion coefficients of the recombining species and *erfc* is the complementary error function. However, there is likely a range of initial distances, r_0, so eq 1 must be convoluted with the distribution of r_0. If we assume a Gaussian radial distribution with a variance of σ, the survival probability is

$$\Omega_g(t) = \int_{r_{xn}}^{\infty} \frac{\exp(-r_0^2/2\sigma^2)}{\sqrt{8\pi^3\sigma^6}} \Omega(r_0,t) 4\pi r_0^2 dr_0 \qquad (2)$$

and this can be integrated to yield the expression for the time dependent survival probability

$$\Omega_g(t) = erfc\left(\frac{r_{xn}}{\sqrt{4D't_g}}\right) + \frac{r_{xn}\exp[-r_{xn}^2/4D'(t+t_g)]}{\sqrt{\pi D'(t+t_g)}} erfc\left(\sqrt{\frac{r_{xn}^2 t}{4D't_g(t+t_g)}}\right) \qquad (3)$$

where $\sigma^2 = 2D't_g$. The maximum of the radial distribution is at $r_0 = 2^{1/2}\sigma$ and the average separation distance given by $\langle r_0 \rangle = (8/\pi)^{1/2}\sigma$.[18]

TABLE 1: Parameters Determined from Fitting Transient Data for Solvated Electrons and Ferrocyanide in Reverse Micelles

IR[a]

ω	r_{xn} (Å)	σ (Å)	$\langle r_0 \rangle$ (Å)
8	5.7	4.1	6.6
12	5.2	5.8	9.3

IR[b]

ω	r_{xn} (Å)	σ (Å)	$\langle r_0 \rangle$ (Å)	r_{max} (Å)
8	5.6	5.7	9.0	11.5
12	5.0	5.8	9.3	17.5

800 nm[c]

ω	k (ps^{-1})	τ (ps)	β	C
8	7.1×10^{-3}	141	1.37	0.29
12	5.3×10^{-3}	189	1.49	0.23

[a] Fit to eq 3. [b] Fit to eq 2, modified with an upper limit to the integral, r_{max}. [c] Fit to eqs 4 and 5, with $\tau = 1/k$.

We have not attempted to fit the bleach recovery in bulk water because the data are too noisy to fit reliably. However, we note that there is very little recovery, and it is similar to previous studies.[24,25] Fitting the RM data to eq 3 results in good fits, and the parameters are listed in Table 1. In both cases the reaction distance, r_{xn}, is between 5 and 6 Å, similar to the values obtained in bulk water. However, the average ejection distance for $\omega = 8$ is 6.6 Å, not much larger than r_{xn}. This suggests that a significant portion of the electrons must immediately recombine, while for $\omega = 12$, $\langle r_0 \rangle = 9.3$ Å and only a small percentage of the electrons are within r_{xn}. If this were the case, the quantum yield of $\omega = 8$ would be significantly smaller than $\omega = 12$. This is not a reasonable result considering that the transient signal does not decrease in magnitude by more than expected (~50%) in going from $\omega = 12$ to $\omega = 8$. Another possibility is the RM confinement is limiting the electron distribution distance. This would have a larger effect for the smaller $\omega = 8$ RM, and would result in faster recombination for a given set of parameters. As an alternative fitting procedure, eq 2 was modified to include an upper limit in the integral, r_{max}. The data were then fit to eq 2 including this upper limit. The results are shown in Table 1. This fitting procedure made no difference in the $\omega = 12$ fit, where $r_{max} \geq 20$ Å gave similar fits without changing the other parameters. This fitting procedure resulted in much more realistic parameters for $\omega = 8$ when r_{max} is 11.5 Å. The effect of r_{max} is to put a limit on the electron ejection distance of 11.5 Å. This distance is similar to the radius of free water estimated for $\omega = 8$ AOT RMs from NMR experiments and MD simulations.[1,60] In light of these results, we fit the $\omega = 12$ data with an upper limit of 17.5 Å, the radius of the free water estimated from NMR experiments.[1] This slightly reduced r_{xn} to 5.0 Å with negligible effect on the remaining parameters. These parameters are reported in Table 1. For both $\omega = 8$ and $\omega = 12$, the electron distribution gives an average distance of ~9 Å, significantly smaller than the 15.5 Å value found in bulk water.[24] This difference is most likely a result of the effects of confinement on the initial electron dynamics. The r_{xn} is similar in bulk water and the $\omega = 12$ RMs, but is somewhat larger in the $\omega = 8$ RMs. With our signal-to-noise ratio, it is unclear if this difference is significant and possibly related to confinement.

Another interesting feature of the fit is that the most realistic parameters were obtained using the bulk diffusion coefficients.[24] Since it is generally assumed that the water molecules are less mobile in RMs than the bulk, and that smaller RMs lead to less mobility, it might be expected that a smaller diffusion coefficient should be used. However, longer time scale quenching studies have reported electron quenching rates similar to bulk water when the quencher resides within the water pool.[9] In this study, the location of the quencher was the primary factor in determining how the quenching rates in RMs compared to bulk water. All attempts to fit the data with significantly smaller diffusion coefficients resulted in unrealistic parameters. It is also apparent from the data that reduced diffusion is not the dominant factor in determining the relative kinetics since the $\omega = 8$ recombination is faster than $\omega = 12$, opposite what would be expected based on the expected relative microviscosity trends. Since ferrocyanide appears to reside in the most bulklike region of the RM,[36] it is not that unexpected that diffusion is not much different than in bulk water. Consistent with this, MD simulations have predicted that a significant portion of the "free" water region has a microviscosity that is similar to that of bulk water.[60]

Solvated Electron Dynamics. The transient absorption at 800 nm is primarily due to the absorption of the solvated electron. As seen in Figure 2, the 800 nm absorption and IR bleach are indistinguishable in bulk water. This indicates that geminate recombination is the primary decay pathway for the electron over the time scale of the experiment. Addition of 2.75 M NaCl results in slightly faster recombination, as expected from previous bulk studies.[24] Fits to the diffusion model, eq 3, were not very unique due to the small decay, but good fits resulted using the same parameters as previously reported.[24] An important result is that recombination is still slower in the presence of 2.75 M NaCl in bulk water than in either RM studied. Since this is larger than the expected ionic strength in the RM water pool,[60] ionic strength can be ruled out as the source of the faster kinetics in the RMs compared to bulk water.

In the RMs, the solvated electron absorption signal decays significantly more than the ferrocyanide IR bleach recovers. This suggests an additional decay pathway for the solvated electron. One possible decay pathway is reaction with AOT headgroups. Radiolysis of dry RMs has shown evidence of electrons reacting with the sulfonate headgroups of AOT.[8] When solvated electrons are formed from multiphoton ionization of isooctane (e.g., without ferrocyanide), a small (12%) decay in the electron signal is observed that is independent of ω. This is similar to what has been observed in previous studies.[4,5] Reaction with AOT is one possible mechanism for this decay. The same process is expected to also occur in the ferrocyanide containing RMs. This could be the origin of the difference between the solvated electron absorption and the ferrocyanide bleach. However, the difference between the transient of the ferrocyanide containing RMs (27% and 20% for $\omega = 8$ and 12, respectively) is larger than the decay in the case without ferrocyanide. This difference could be due to the K^+ counterions of ferrocyanide shielding the negative charge of AOT in the high ionic strength environment. As was the case for geminate recombination, the additional electron reactivity is larger for $\omega = 8$ than $\omega = 12$, the opposite of what would be expected if changes in the microviscosity were dominant.

To quantify the additional decay component, we have fit the 800 nm solvated electron absorption to a function that includes the fit of the IR bleach data plus an additional decay component. The functional form is

$$\Delta A_{800}(t) = \Omega_g(t) + C[F(t) - 1] \qquad (4)$$

where $F(t)$ represents the additional decay component and C represents the percentage of the initially formed electrons that undergo this decay mechanism. We found that a satisfactory

fit was obtained using a compressed exponential, that is

$$F(t) = e^{-(kt)^{\beta}} \quad (5)$$

where $\beta > 1$. When $\beta < 1$ this expression results in the more commonly encountered stretched exponential function, often attributed to a distribution of lifetimes. We are not ascribing a meaning to this functional form, but are using it only phenomenologically to characterize the kinetic behavior. The time dependence most likely originates from diffusion of the electron to the RM wall. The fit parameters are listed in Table 1. This additional component has a faster rate and larger magnitude for $\omega = 8$ than $\omega = 12$, while β is similar for both. This is consistent with the intuitively appealing faster reactivity in the smaller RM. Attempts were made to use several other functional forms. An equally good fit was obtained using an exponential decay with a delay onset of ~50 ps, but we chose to use the compressed exponential. We also tried summing the decays from the IR bleach recovery with the 800 nm decay from the RMs without ferrocyanide. This resulted in poor fits or unrealistic parameters. This indicates that the additional decay component in the ferrocyanide containing RMs has different kinetics, as well as having a larger magnitude, than the electron decay in the absence of ferrocyanide. This does not necessarily imply a different mechanism. The mechanism could be the same in both cases with the different kinetic behavior originating in the increased ionic strength when ferrocyanide is included.

Overall it appears that diffusion of the electron is not significantly slowed in AOT RMs. This is in contrast to previous experiments that have shown slower diffusion and reduced overall solute mobility in RM water pools than in bulk water.[36,61−68] The mobility appears to depend on both the location of the solute in the RM as well as on the solute size.[36,65,66,68] The solute size can also influence the solute location. A smaller solute can sample a smaller region of the RM interior and a smaller charged solute is generally more hydrophilic than a larger solute of the same charge. The solvated electron is very small and very hydrophilic, enabling the electron to reside in the most polar bulklike region of the RM rather than the more restricted outer regions, as indicated by our determined $\langle r_0 \rangle$ values, which are within the bulklike core region of the RM.[1,60] It is unclear if the mobility of the solvated electron is due to its small size or it location in a bulklike region of the RM.

Conclusions

Solvated electrons have been created through photodetachment of ferrocyanide in AOT reverse micelles. The geminate recombination process has been probed via the ferrocyanide CN stretching band in the infrared and faster recombination is observed in RMs than in bulk water with faster recombination for smaller RMs. This faster recombination is not due to ionic strength effects. Using a diffusion model to fit the geminate recombination kinetics results in parameters that are similar to those in the bulk with the exception of the electron distribution. A narrower distribution occurs in the RMs, as may be expected due to the confinement effects of the RM. The same parameters fit both RM systems, $\omega = 8$ and $\omega = 12$, with the addition of an upper limit on the electron-ferrocyanide separation distance of 11.5 Å for $\omega = 8$. Realistic parameters are extracted from the fit only when the diffusion coefficient is similar to that of bulk water, implying that diffusion of the solvated electron is not significantly inhibited by RM confinement.

Probing the solvated electron directly at 800 nm resulted in different kinetics than the IR probe. There was an additional decay component evident in the 800 nm data that was larger for the smaller RM. This is in contrast to the results in bulk water where the IR and 800 nm data are identical within experimental error. The additional component is tentatively assigned to reaction of the solvated electron with the headgroups of AOT. Multiphoton ionization of RMs without ferrocyanide also leads to solvated electrons that exhibit a small decay over a 300 ps time window, but it is smaller than the additional decay component in the ferrocyanide containing RMs. The difference in the two cases could be due to ionic strength effects rather than a different mechanism of solvated electron decay.

Acknowledgment. Support for this work was provided by the Office of Naval Research through the Naval Research Laboratory. G.M.S. acknowledges the Naval Research Laboratory—American Society for Engineering Education Postdoctoral Fellowship program.

References and Notes

(1) Maitra, A. *J. Phys. Chem.* **1984**, *88*, 5122.
(2) Brubach, J. B.; Mermet, A.; Filabozzi, A.; Gerschel, A.; Lairez, D.; Krafft, M. P.; Roy, P. *J. Phys. Chem. B* **2001**, *105*, 430.
(3) Garrett, B. C.; Dixon, D. A.; Camaioni, D. M.; Chipman, D. M.; Johnson, M. A.; Jonah, C. D.; Kimmel, G. A.; Miller, J. H.; Rescigno, T. N.; Rossky, P. J.; Xantheas, S. S.; Colson, S. D.; Laufer, A. H.; Ray, D.; Barbara, P. F.; Bartels, D. M.; Becker, K. H.; Bowen, H.; Bradforth, S. E.; Carmichael, I.; Coe, J. V.; Corrales, L. R.; Cowin, J. P.; Dupuis, M.; Eisenthal, K. B.; Franz, J. A.; Gutowski, M. S.; Jordan, K. D.; Kay, B. D.; LaVerne, J. A.; Lymar, S. V.; Madey, T. E.; McCurdy, C. W.; Meisel, D.; Mukamel, S.; Nilsson, A. R.; Orlando, T. M.; Petrik, N. G.; Pimblott, S. M.; Rustad, J. R.; Schenter, G. K.; Singer, S. J.; Tokmakoff, A.; Wang, L. S.; Wittig, C.; Zwier, T. S. *Chem. Rev.* **2005**, *105*, 355.
(4) Lee, Y. J.; Kee, T. W.; Zhang, T. Q.; Barbara, P. F. *J. Phys. Chem. B* **2004**, *108*, 3474.
(5) Lee, Y. J.; Zhang, T. Q.; Barbara, P. F. *J. Phys. Chem. B* **2004**, *108*, 5175.
(6) Calvo-Perez, V.; Beddard, G. S.; Fendler, J. H. *J. Phys. Chem.* **1981**, *85*, 2316.
(7) Gauduel, Y.; Pommeret, S.; Yamada, N.; Migus, A.; Antonetti, A. *J. Am. Chem. Soc.* **1989**, *111*, 4974.
(8) Gebicki, J. L.; Gebicka, L.; Kroh, J. *J. Chem. Soc., Faraday Trans.* **1994**, *90*, 3411.
(9) Adhikari, S.; Joshi, R.; Gopinathan, C. *Int. J. Chem. Kinet.* **1998**, *30*, 699.
(10) Gebicki, J. L.; Maciejewska, M. *Radiat. Phys. Chem.* **2003**, *67*, 257.
(11) Pileni, M. P.; Hickel, B.; Ferradini, C.; Pucheault, J. *Chem. Phys. Lett.* **1982**, *92*, 308.
(12) Joshi, R.; Mukherjee, T. *Radiat. Phys. Chem.* **2003**, *66*, 397.
(13) Bakale, G.; Beck, G.; Thomas, J. K. *J. Phys. Chem.* **1981**, *85*, 1062.
(14) Wong, M.; Gratzel, M.; Thomas, J. K. *Chem. Phys. Lett.* **1975**, *30*, 329.
(15) Kee, T. W.; Son, D. H.; Kambhampati, P.; Barbara, P. F. *J. Phys. Chem. A* **2001**, *105*, 8434.
(16) Vilchiz, V. H.; Kloepfer, J. A.; Germaine, A. C.; Lenchenkov, V. A.; Bradforth, S. E. *J. Phys. Chem. A* **2001**, *105*, 1711.
(17) Kloepfer, J. A.; Vilchiz, V. H.; Lenchenkov, V. A.; Chen, X. Y.; Bradforth, S. E. *J. Chem. Phys.* **2002**, *117*, 766.
(18) Kloepfer, J. A.; Vilchiz, V. H.; Lenchenkov, V. A.; Germaine, A. C.; Bradforth, S. E. *J. Chem. Phys.* **2000**, *113*, 6288.
(19) Iglev, H.; Laenen, R.; Laubereau, A. *Chem. Phys. Lett.* **2004**, *389*, 427.
(20) Assel, M.; Laenen, R.; Laubereau, A. *Chem. Phys. Lett.* **1998**, *289*, 267.
(21) Long, F. H.; Lu, H.; Eisenthal, K. B. *J. Chem. Phys.* **1989**, *91*, 4413.
(22) Long, F. H.; Lu, H.; Shi, X. L.; Eisenthal, K. B. *Chem. Phys. Lett.* **1990**, *169*, 165.
(23) Crowell, R. A.; Lian, R.; Shkrob, I. A.; Bartels, D. M.; Chen, X. Y.; Bradforth, S. E. *J. Chem. Phys.* **2004**, *120*, 11712.
(24) Lenchenkov, V.; Kloepfer, J.; Vilchiz, V.; Bradforth, S. E. *Chem. Phys. Lett.* **2001**, *342*, 277.
(25) Anderson, N. A.; Hang, K.; Asbury, J. B.; Lian, T. Q. *Chem. Phys. Lett.* **2000**, *329*, 386.
(26) Pommeret, S.; Naskrecki, R.; van der Meulen, P.; Menard, M.; Vigneron, G.; Gustavsson, T. *Chem. Phys. Lett.* **1998**, *288*, 833.
(27) Shirom, M.; Stein, G. *J. Chem. Phys.* **1971**, *55*, 3372.

(28) Matheson, M. S.; Mulac, W. A.; Rabani, J. *J. Phys. Chem.* **1963**, *67*, 2613.
(29) Sauer, M. C.; Shkrob, I. A.; Lian, R.; Crowell, R. A.; Bartels, D. M.; Chen, X. Y.; Suffern, D.; Bradforth, S. E. *J. Phys. Chem. A* **2004**, *108*, 10414.
(30) Crowell, R. A.; Bartels, D. M. *J. Phys. Chem.* **1996**, *100*, 17940.
(31) Kambhampati, P.; Son, D. H.; Kee, T. W.; Barbara, P. F. *J. Phys. Chem. A* **2002**, *106*, 2374.
(32) Laenen, R.; Roth, T.; Laubereau, A. *Phys. Rev. Lett.* **2000**, *85*, 50.
(33) Shi, X. L.; Long, F. H.; Lu, H.; Eisenthal, K. B. *J. Phys. Chem.* **1996**, *100*, 11903.
(34) Hertwig, A.; Hippler, H.; Unterreiner, A. N. *Phys. Chem. Chem. Phys.* **1999**, *1*, 5633.
(35) Pshenichnikov, M. S.; Baltuska, A.; Wiersma, D. A. *Chem. Phys. Lett.* **2004**, *389*, 171.
(36) Sando, G. M.; Dahl, K.; Owrutsky, J. C. *J. Phys. Chem. B* **2005**, *109*, 4084.
(37) Bohidar, H. B.; Behboudnia, M. *Colloids Surf., A* **2001**, *178*, 313.
(38) Jain, T. K.; Varshney, M.; Maitra, A. *J. Phys. Chem.* **1989**, *93*, 7409.
(39) Onori, G.; Santucci, A. *J. Phys. Chem.* **1993**, *97*, 5430.
(40) Levinger, N. E. *Curr. Opin. Colloid Interface Sci.* **2000**, *5*, 118.
(41) Harpham, M. R.; Ladanyi, B. M.; Levinger, N. E.; Herwig, K. W. *J. Chem. Phys.* **2004**, *121*, 7855.
(42) Zhong, Q.; Baronavski, A. P.; Owrutsky, J. C. *J. Chem. Phys.* **2003**, *118*, 7074.
(43) Gehlen, M. H.; Deschryver, F. C. *Chem. Rev.* **1993**, *93*, 199.
(44) Sauer, M. C.; Crowell, R. A.; Shkrob, I. A. *J. Phys. Chem. A* **2004**, *108*, 5490.
(45) Cavanagh, M. C.; Martini, I. B.; Schwartz, B. J. *Chem. Phys. Lett.* **2004**, *396*, 359.
(46) Assel, M.; Laenen, R.; Laubereau, A. *J. Chem. Phys.* **1999**, *111*, 6869.
(47) Assel, M.; Laenen, R.; Laubereau, A. *J. Phys. Chem. A* **1998**, *102*, 2256.
(48) Crowell, R. A.; Lian, R.; Shkrob, I. A.; Qian, J.; Oulianov, D. A.; Pommeret, S. *J. Phys. Chem. A* **2004**, *108*, 9105.
(49) Lian, R.; Oulianov, D. A.; Shkrob, I. A.; Crowell, R. A. *Chem. Phys. Lett.* **2004**, *398*, 102.
(50) Sander, M. U.; Gudiksen, M. S.; Luther, K.; Troe, J. *Chem. Phys.* **2000**, *258*, 257.
(51) Hertwig, A.; Hippler, H.; Unterreiner, A. N. *Phys. Chem. Chem. Phys.* **2002**, *4*, 4412.
(52) Bartels, D. M.; Crowell, R. A. *J. Phys. Chem. A* **2000**, *104*, 3349.
(53) Thaller, A.; Laenen, R.; Laubereau, A. *Chem. Phys. Lett.* **2004**, *398*, 459.
(54) Webster, F. J.; Schnitker, J.; Friedrichs, M. S.; Friesner, R. A.; Rossky, P. J. *Phys. Rev. Lett.* **1991**, *66*, 3172.
(55) Siebbeles, L. D. A.; Emmerichs, U.; Hummel, A.; Bakker, H. J. *J. Chem. Phys.* **1997**, *107*, 9339.
(56) Sander, M. U.; Brummund, U.; Luther, K.; Troe, J. *J. Phys. Chem.* **1993**, *97*, 8378.
(57) Zhang, T. Q.; Lee, Y. J.; Kee, T. W.; Barbara, P. F. *Chem. Phys. Lett.* **2005**, *403*, 257.
(58) Hankiewicz, E.; Schultefrohlinde, D. *J. Phys. Chem.* **1977**, *81*, 2614.
(59) Capone, S.; Derobertis, A.; Sammartano, S.; Rigano, C. *Thermochim. Acta* **1986**, *102*, 1.
(60) Faeder, J.; Ladanyi, B. M. *J. Phys. Chem. B* **2000**, *104*, 1033.
(61) Saez, M.; Abuin, E. A.; Lissi, E. A. *Langmuir* **1989**, *5*, 942.
(62) Riter, R. E.; Willard, D. M.; Levinger, N. E. *J. Phys. Chem. B* **1998**, *102*, 2705.
(63) Pant, D.; Levinger, N. E. *Langmuir* **2000**, *16*, 10123.
(64) Hazra, P.; Chakrabarty, D.; Chakraborty, A.; Sarkar, N. *Chem. Phys. Lett.* **2003**, *382*, 71.
(65) Dutt, G. B. *J. Phys. Chem. B* **2004**, *108*, 7944
(66) Dutt, G. B. *J. Phys. Chem. B* **2004**, *108*, 805.
(67) Zhong, Q.; Baronavski, A. P.; Owrutsky, J. C. *J. Chem. Phys.* **2003**, *119*, 9171.
(68) Sando, G. M.; Dahl, K.; Owrutsky, J. C. *J. Phys. Chem. A* **2004**, *108*, 11209.